Electronic Journal of Polish Agricultural Universities is the very first Polish scientific journal published exclusively on the Internet, founded on January 1, 1998 by the following agricultural universities and higher schools of agriculture: University of Technology and Agriculture of Bydgoszcz, Agricultural University of Cracow, Agricultural University of Lublin, Agricultural University of Poznan, Higher School of Agriculture and Teacher Training Siedlce, Agricultural University of Szczecin, and Agricultural University of Wroclaw.

ELECTRONIC JOURNAL OF POLISH AGRICULTURAL UNIVERSITIES

2004
Volume 7
Issue 2
Series CIVIL ENGINEERING

DOBISZEWSKA M. PROBLEM OF COUPLED THERMOELASTICITY IN ELASTIC RIGID DISKS
Electronic Journal of Polish Agricultural Universities, Civil Engineering, Volume 7, Issue 2.
Available Online http://www.ejpau.media.pl

PROBLEM OF COUPLED THERMOELASTICITY IN ELASTIC RIGID DISKS

Magdalena Dobiszewska
Department of Structural Mechanics, University of Technology and Agriculture, Bydgoszcz, Poland

ABSTRACT

The paper presents a problem of coupled thermoelasticity in elastic rigid disks. To solve this problem, two numerical methods have been applied. First of all, a finite elements method was used and as result of it the set of ordinary differential equations with regard to a time variable was obtained. This set of equations was solved with the second numerical method – SSpj method. On the basis of carried out calculations, short qualitative analysis of the influence of the field of strains and temperature coupling on generation and character of displacements, stresses and temperature fields was determined.

Key words: coupled thermoelasticity, rigid disk, finite elements method, Zienkiewicz-Wood's (SSpj) method.

1. INTRODUCTION

The subject of this paper is a problem of initially-edged coupled thermoelasticity in rigid disks which are under influence of a time and space variable external load $p(\mathrm{X},t)$ and thermal interaction $\hat{\Theta}(\mathrm{X},t)$. B denotes the interior of the rigid disk, but $\partial\mathrm{B}$ denotes its boundary area, which parts are distinguished by known loads - $\partial\mathrm{B}_{\mathrm{p}}$ and displacements- $\partial\mathrm{B}_{\mathrm{u}}$ as well as the parts, where the thermal boundary conditions $\partial\mathrm{B}_1$ - of the first, $\partial\mathrm{B}_2$ - the second and $\partial\mathrm{B}_3$ - of the third kind are known. Considerations presented in the paper refer to isotropic,

homogenous, geometrically and physically linear conditions. Change of temperature in the considered rigid disk is so small, that does not cause any essential changes in material, thermal and elastic coefficients. With such a range of temperature changes the influence of the field of strains with the field of temperature coupling with respect to qualitative analysis is very small and practically, can be neglected. The qualitative analysis of the coupling between these fields and research of the coupling influence on the character of generated fields of strains, stresses and temperature is the main problem of this paper.

Fig. 1. Considered rigid disk

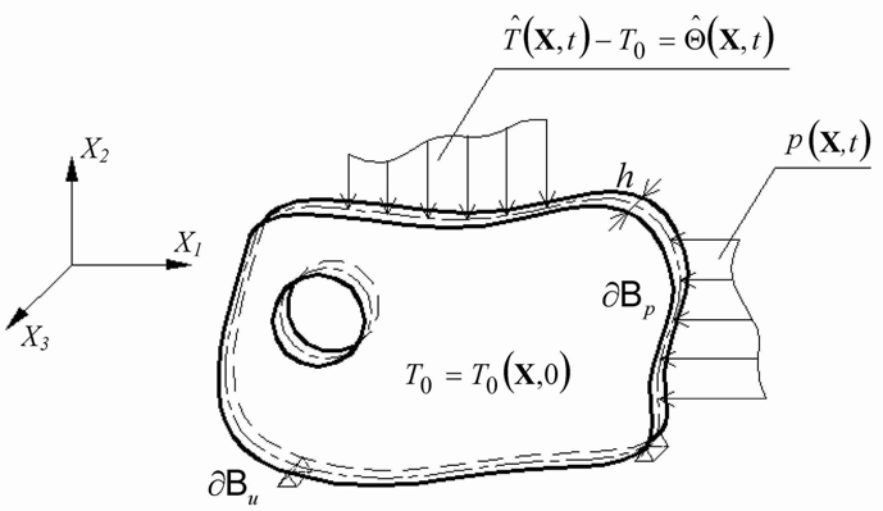

2. THE EQUATION OF COUPLED THERMOELASTICITY IN RIGID DISKS

Considering different kinds of thermal boundary conditions, the virtual work equations of coupled thermoelasticity in elastic, rigid disks one may present in the shape of two equations [1]:

$$\int_B \rho f_i \delta u_i dB + \int_{\partial B_p} p_i \delta u_i d(\partial B) - \int_B \rho \ddot{u}_i \delta u_i dB =$$

$$= \int_B \left(2\mu \varepsilon_{ij} \delta \varepsilon_{ij} + \frac{2\mu\nu}{1-\nu} e_* \delta \varepsilon_{kk} \right) dB + \frac{1-2\nu}{1-\nu} \gamma \int_B \Theta \delta \varepsilon_{kk} dB = 0,$$

$$\left(\frac{c_\varepsilon}{T_0} + \frac{1+\nu}{1-\nu} \gamma \alpha_t \right) \int_B \Theta \delta \Theta \, dB + \vartheta \frac{1-2\nu}{1-\nu} \gamma \int_B \Theta \delta e_* dB - \int_B \Theta \delta \tau \, dB + \frac{1}{T_0} \int_B \Theta \delta \omega dB + \tag{2.1}$$

$$\frac{T_0}{\lambda_0} \int_B \dot{H}_i \delta H_i \, dB + \int_{\partial B_1} g_i \delta H_i d(\partial B) + \int_{\partial B_2} \left(\Theta n_i + \frac{\lambda_0}{\alpha} \Theta_{,i} \right) \delta H_i d(\partial B) +$$

$$\int_{\partial B_2} k_i \delta H_i d(\partial B) - \frac{\lambda_0}{\alpha} \int_{\partial B_3} \Theta_{,i} \delta H_i d(\partial B) + \int_{\partial B_3} m_i \delta H_i d(\partial B) = 0,$$

i,j,k = 1,2,

where:

ε_{ij} - components of the strain tensor, u_i - component of the displacement vector, ρ - density, f_i - intensity of mass forces per mass unit, $\ddot{u}_i$ - components of the displacement acceleration vector, $e_* = \varepsilon_{11} + \varepsilon_{22} = const$ - dilatation, relative change of volume, $\Theta = T - T_0$ - change of temperature, T_0 - initial temperature, p_i - components of the load vector, H_i - Biot's vector components, [$JK^{-1}m^{-2}$], μ, λ - Lamé's constants of the material, ν - Poisson's ratio, γ - coefficient proportional to specific heat by constant deformation, [$JK^{-1}m^{-3}$], λ_0 - coefficient of thermal conductivity, [$WK^{-1}m^{-1}$], α - surface film conductance, [$WK^{-1}m^{-2}$], c_ε - specific

heat by constant deformation, [JK^{-1}m^{-3}], $\tau = \frac{\lambda_0}{T_0}\varepsilon_0 \int_0^t \widetilde{\Theta}\, dt + \tau_0$, [JK^{-1}m^{-3}], $\varepsilon_0 = \frac{2\alpha}{h\lambda_0}$, [m^{-2}], $\widetilde{\Theta} = \hat{T} - T$ - difference of temperatures between the surrounding medium and surface of the rigid disk, h - rigid disk thickness, $\omega = \int_0^t W\, dt + \omega_0$ -global quantity of heat emitted by a volume unit from the time instant *t=0* to time *t*, [Jm^{-3}], ω_0 - initial heat quantity, [Jm^{-3}], W - caloric effect of internal heat sources, [Wm^{-3}], n_j - direction cosine of an angle between a normal to considered boundary area and the X_j axis, $g_i = \hat{\Theta} n_i$ - function given at the surface $\partial \mathrm{B}_1$, $\hat{\Theta} = \hat{T} - T_0$, $\hat{T}$ - temperature of the fluid surrounding the body, $k_i = \frac{1}{\alpha}\hat{q}_i$ - function given at the surface $\partial \mathrm{B}_2$, $\hat{q}_i$ - component of the stream heat density vector at the body surface, [W m^{-2}], $m_i = \hat{\Theta} n_i$ - function given for the surface $\partial \mathrm{B}_3$, $f_{,k} = \frac{\partial f}{\partial X_k}$.

Equation $(2.1)_1$ constitutes a generalised principle of Lagrange`s virtual work on a problem of thermoelasticity, but relation $(2.1)_2$ describes the equation of virtual work of heat conductivity. The second variation equation has been derived with taking account the internal heat sources and the admission of possibilities to change the thermal boundary conditions at planes limiting the rigid disk $X_3 = \pm h/2$. An additional assumption that the temperature distribution is symmetrical with respect to the central area of the rigid disk was made. In the case, when temperature action is such that its variation appears only in a plane of the rigid disk, the parameter $\varepsilon_0 = 0$ ought to be assumed. It means, that in a direction perpendicular to the rigid disk there is no heat exchange and the rigid disk at the planes $X_3 = \pm h/2$ is thermally isolated. The virtual work equation of thermoelasticity presented in the paper for different types of thermal boundary conditions at the edges of the rigid disk have been considered as well. The coupling of deformation field with the field of temperatures represents the integral:

$\frac{1-2\nu}{1-\nu}\gamma \int_{\mathrm{B}} \Theta \delta e_* \, d\mathrm{B}$, existing in the equation of virtual work of heat conductivity, which is additionally denoted by a parameter ϑ. Setting this integral to zero causes de-coupling of these fields.

3. EQUATION OF MOTION IN FINITE ELEMENTS METHOD

In further considerations, the internal sources of heat have been neglected and the assumption that the rigid disk at the planes $X_3 = \pm h/2$ is thermally isolated, i.e. $\varepsilon_0 = 0$ was taken. All the components of virtual work equations (2.1) and (2.2) for a finite element (FE) are described as in the following:

- displacements

$$u_i^e = \phi_{i\alpha}^e r_\alpha, \tag{3.1}$$

- strains

$$\varepsilon_{ij}^e = B_{ij\alpha}^e r_\alpha, \quad B_{ij\alpha}^e = \frac{1}{2}\left(\phi_{i\alpha,j}^e + \phi_{j\alpha,i}^e\right) \tag{3.2}$$

- Biot's vector

$$H_i^e = \phi_{i\alpha}^e h_\alpha, \tag{3.3}$$

- temperature

$$\Theta^e = A_{i\alpha,i}^e h_\alpha + \vartheta \widetilde{B}_{kk\alpha}^e r_\alpha, \tag{3.4}$$

$$A^e_{i\alpha,i} = -\frac{1}{\dfrac{1+\nu^e}{1-\nu^e}\alpha^e_t\gamma^e + \dfrac{c^e_\varepsilon}{T^e_0}}\phi^e_{i\alpha,i}, \quad \widetilde{B}^e_{kk\alpha} = -\frac{\dfrac{1-2\nu^e}{1-\nu^e}}{\dfrac{1+\nu^e}{1-\nu^e}\alpha^e_t\gamma^e + \dfrac{c^e_\varepsilon}{T^e_0}}\gamma^e B^e_{kk\alpha},$$

$$\boldsymbol{X}, T, t \in \Omega_e \times \langle T_0, T_1\rangle \times \langle 0, \infty), \quad \text{i} = 1,2,$$

where:

$(\boldsymbol{X}, T, t) \in \Omega_e \times \langle T_0, T_1\rangle \times \langle 0, \infty)$, i = 1,2,

$\phi^e_{i\alpha} = \phi^e_{i\alpha}(\mathbf{X})$ - function of shape, $r_\alpha = r_\alpha(t)$ - parameters, displacements of joints, $h_\alpha = h_\alpha(t)$ - Biot's vector joint parameters, ϑ - parameter which considers fields of deformation and temperature coupling, Ω_e - FE, $e = 1, 2, \ldots, E$ - number of FE, $\alpha = 1, 2, \ldots, \Lambda$, $\Lambda = w \cdot s$ - number of degrees of freedom in FE joints, E - number of FE, w - number of FE joints, s - number of degrees of freedom in a joint.

Substituting relations (3.1)÷(3.4) to virtual work equations (2.1) i (2.2) and considering that the variation of displacement δu_i and Biot's vector variations δH_i are arbitrary in FE region, one obtained the equations of motion:

$$\begin{aligned}
&\sum_{e=1}^{E}\left[\mathbf{M}^e_{\alpha\beta}\ddot{\mathbf{r}}_\alpha + \left(\mathbf{K}^e_{\alpha\beta} + \mathbf{V}^e_{\alpha\beta}\right)\mathbf{r}_\alpha + \mathbf{T}^e_{\alpha\beta}\mathbf{h}_\alpha - \mathbf{R}^e_\beta\right] = 0,\\
&\sum_{e=1}^{E}\Big[\mathbf{L}^e_{\alpha\beta}\dot{\mathbf{h}}_\alpha + \left(\mathbf{S}^e_{\alpha\beta} + \mathbf{Q}^e_{\alpha\beta} + \mathbf{G}^e_{\alpha\beta} - \mathbf{I}^e_{\alpha\beta}\right)\mathbf{h}_\alpha +\\
&+\vartheta\left(\mathbf{W}^e_{\alpha\beta} + \mathbf{Z}^e_{\alpha\beta} + \mathbf{H}^e_{\alpha\beta} - \mathbf{J}^e_{\alpha\beta}\right)\mathbf{r}_\alpha + \left(\mathbf{E}^e_\beta + \mathbf{N}^e_\beta + \mathbf{O}^e_\beta\right)\Big] = 0
\end{aligned} \tag{3.5}$$

or in an integrated form:

$$\sum_{e=1}^{E}\left\{\mathtt{M}^{\,e}\ddot{\mathbf{X}} + \mathtt{C}^{\,e}\dot{\mathbf{X}} + \mathtt{K}^{\,e}\mathbf{X} - \mathtt{P}^{\,e}\right\} = \mathbf{0}, \tag{3.6}$$

where:

$$\mathtt{M}^{\,e} = \begin{bmatrix}\mathbf{M}^e & \mathbf{0}\\ \mathbf{0} & \mathbf{0}\end{bmatrix}, \quad \mathtt{C}^{\,e} = \begin{bmatrix}\mathbf{0} & \mathbf{0}\\ \mathbf{0} & \mathbf{L}^e\end{bmatrix}, \quad \mathtt{P}^{\,e} = \begin{bmatrix}\mathbf{R}^e\\ -\mathbf{E}^e - \mathbf{N}^e - \mathbf{O}^e\end{bmatrix},$$
$$\mathtt{K}^{\,e} = \begin{bmatrix}\mathbf{K}^e + \mathbf{V}^e & \mathbf{T}^e\\ \vartheta\left(\mathbf{W}^e + \mathbf{Z}^e + \mathbf{H}^e - \mathbf{J}^e\right) & \mathbf{S}^e + \mathbf{Q}^e + \mathbf{G}^e - \mathbf{I}^e\end{bmatrix}. \tag{3.7}$$

Individual elements of the matrix describe the integrals that resulted from integration over the whole range of FE

$$\begin{aligned}
&M^e_{\alpha\beta} = \int_{\Omega_e}\rho^e\Phi^e_{i\alpha}\Phi^e_{i\beta}d\Omega, \quad K^e_{\alpha\beta} = \int_{\Omega_e}\left(2\mu^e B^e_{ij\alpha}B^e_{ij\beta} + \frac{2\mu^e\nu^e}{1-\nu^e}B^e_{ii\alpha}B^e_{jj\beta}\right)d\Omega,\\
&L^e_{\alpha\beta} = \frac{T^e_o}{\lambda^e_0}\int_{\Omega_e}\Phi^e_{i\alpha}\Phi^e_{i\beta}d\Omega = \frac{T^e_o}{\lambda^e_0\rho^e}M^e_{\alpha\beta}, \quad S^e_{\alpha\beta} = \left(\frac{c^e_\varepsilon}{T^e_0} + \frac{1+\nu}{1-\nu}\gamma^e\alpha^e_t\right)\int_{\Omega_e}A^e_{i\alpha,i}A^e_{j\beta,j}d\Omega,\\
&T^e_{\alpha\beta} = \left(\frac{c^e_\varepsilon}{T^e_0} + \frac{1+\nu}{1-\nu}\gamma^e\alpha^e_t\right)\int_{\Omega_e}A^e_{i\alpha,i}\widetilde{B}^e_{rr\beta}d\Omega, \quad W^e_{\alpha\beta} = \left(\frac{c^e_\varepsilon}{T^e_0} + \frac{1+\nu}{1-\nu}\gamma^e\alpha^e_t\right)\int_{\Omega_e}\widetilde{B}^e_{kk\alpha}A^e_{j\beta,j}d\Omega,\\
&V^e_{\alpha\beta} = \left(\frac{c^e_\varepsilon}{T^e_0} + \frac{1+\nu}{1-\nu}\gamma^e\alpha^e_t\right)\int_{\Omega_e}\widetilde{B}^e_{kk\alpha}\widetilde{B}^e_{rr\beta}d\Omega
\end{aligned} \tag{3.8}$$

and resulting from integration along the edges of FE

$$Q^e_{\alpha\beta} = \int_{\partial\Omega_{e2}} A^e_{j\alpha,j} n^e_i \Phi^e_{i\beta} d(\partial\Omega), \quad Z^e_{\alpha\beta} = \int_{\partial\Omega_{e2}} \widetilde{B}^e_{kk\alpha} n^e_i \Phi^e_{i\beta} d(\partial\Omega),$$
$$G^e_{\alpha\beta} = \frac{\lambda^e_0}{\alpha^e} \int_{\partial\Omega_{e2}} A^e_{j\alpha,ji} \Phi^e_{i\beta} d(\partial\Omega), \quad H^e_{\alpha\beta} = \frac{\lambda^e_0}{\alpha^e} \int_{\partial\Omega_{e2}} \widetilde{B}^e_{kk\alpha} \Phi^e_{i\beta} d(\partial\Omega), \tag{3.9}$$
$$I^e_{\alpha\beta} = \frac{\lambda^e_0}{\alpha^e} \int_{\partial\Omega_{e3}} A^e_{j\alpha,ji} \Phi^e_{i\beta} d(\partial\Omega), \quad J^e_{\alpha\beta} = \frac{\lambda^e_0}{\alpha^e} \int_{\partial\Omega_{e3}} \widetilde{B}^e_{kk\alpha,i} \Phi^e_{i\beta} d(\partial\Omega)$$

and integrals which describe the impulse of joints

$$R^e_\beta = \int_{\Omega_e} \rho^e f^e_i \Phi^e_{i\beta} d\Omega + \int_{\partial\Omega_{ep}} p^e_i \Phi^e_{i\beta} d(\partial\Omega), \quad E^e_\beta = \int_{\partial\Omega_{e1}} g^e_i \Phi^e_{i\beta} d(\partial\Omega), \tag{3.10}$$
$$N^e_\beta = \int_{\partial\Omega_{e2}} k^e_i \Phi^e_{j\beta} d(\partial\Omega), \quad O^e_\beta = \int_{\partial\Omega_{e3}} m^e_i \Phi^e_{j\beta} d(\partial\Omega).$$

After aggregation along FE, the following equations of motion are obtained:

$$\mathbf{M}\ \ddot{\mathbf{X}} + \mathbf{C}\dot{\mathbf{X}} + \mathbf{K}\,\mathbf{X} = \mathbf{P}\ . \tag{3.11}$$

The parameter $\vartheta = 1$ is for coupled processes, but in the case when $\vartheta = 0$ a de-coupled process appears.

4. SOLUTION TO EQUATIONS OF MOTION BY SSPJ METHOD

Zienkiewicz-Wood's method, called also SSpj method (SSpj – single step algorithm) belongs to direct integration methods and is used for numerical solving of ordinary differential equations [2,3]. This method was applied for solving equations of motion (3.11), where the unknown function $X(t)$ in consecutive discreted points at the time axis was in search. In the said method, a parameter *j* denotes a row of solved differential equations, and parameter *p* denotes a number of elements of the expansion of solved differential equations in to a power series. Equation of motion (3.11) can be solved by taking advantage of arbitrary alternative of SS_{pj} method [4]. A recurrence procedure, e. g. for alternative of SS_{22} method (quadratic algorithm) is as follows:

$$\boldsymbol{\alpha}^{(2)}_{\mathrm{i}} = \left[\mathbf{M} + \Delta t\Theta_1\mathbf{C} + 0{,}5(\Delta t)^2\Theta_2\mathbf{K}\right]^{-1}\left[\overline{\mathbf{P}} - \mathbf{C}\dot{\widetilde{\mathbf{X}}}_{\mathrm{i+1}} - \mathbf{K}\,\widetilde{\mathbf{X}}_{\mathrm{i+1}}\right],$$
$$\widetilde{\mathbf{X}}_{\mathrm{i+1}} = \mathbf{X}_{\mathrm{i}} + \Theta_1\Delta t\dot{\mathbf{X}}_{\mathrm{i}}, \quad \dot{\widetilde{\mathbf{X}}}_{\mathrm{i+1}} = \dot{\mathbf{X}}_{\mathrm{i}},$$
$$\mathbf{X}_{\mathrm{i+1}} = \mathbf{X}_{\mathrm{i}} + \Delta t\dot{\mathbf{X}}_{\mathrm{i}} + \boldsymbol{\alpha}^{(2)}_{\mathrm{i}}\frac{(\Delta t)^2}{2}, \quad \dot{\mathbf{X}}_{\mathrm{i+1}} = \dot{\mathbf{X}}_{\mathrm{i}} + \boldsymbol{\alpha}^{(2)}_{\mathrm{i}}\Delta t\ , \tag{3.12}$$
$$\mathrm{i}=0,\ 1,\ 2,\ \ldots,\ \mathrm{T},$$

where Δt indicates an integration step and Θ_i are parameters of the method. Algorithm SS_{22} in form (3.12) is unconditionally stable, if the parameters Θ_1 and Θ_2 fulfil the following conditions [2,3]:

$$\Theta_1 \geq 0{,}5, \qquad \Theta_2 \geq \Theta_1. \tag{3.13}$$

5. EXAMPLES OF CALCULATIONS

Using a finite elements method for solving the problem of rigid disks, a discretation to rectangular finite elements, which have two degrees of freedom in each corner of joints, are accomplished. In calculations, a linear function of shape was applied. Equation of motion (3.11) was solved using a variant of SS_{22} method, whose recurrence procedure in relations (3.12) was presented. The following data were assumed, with regard to:

a) elastic properties of rigid disk materials: Young's modulus $E = 208$ GPa, Poisson's ratio $\nu = 0.3$, Kirchhoff's modulus $G = \mu = 80$ GPa, Lame`s constant, $\lambda = 120$ GPa,

b) thermal properties of rigid disk materials: coefficient of thermal conductivity $\lambda_0 = 0{,}0503$ kW $K^{-1}m^{-1}$, specific heat by constant deformation, $c_\varepsilon = 3\,575.5$ $kJK^{-1}m^{-3}$, coefficient of linear thermal expansion $\alpha_t = 12 \cdot 10^{-6}$ K^{-1}, coefficient proportional to entropy - $\gamma = \frac{2\mu\,(1+\nu)}{(1-2\nu)}\alpha_t = 6\,240$ kN $K^{-1}m^{-2}$.

The initial conditions relative to displacements and velocity of displacements i.e. $u_i(X_1,X_2) = 0$, $\dot{u}_i(X_1,X_2) = 0$ (where i = 1, 2) and applying to internal temperature $T_0(X_1,X_2) = T_0$ were assumed. The boundary conditions were formulated in analysed below examples.

Example 1

A rigid disk of an elongated shape, unilaterally fixed, rapidly loaded by external temperature $\Theta_z(t) = \hat{\Theta}(t) = \hat{\Theta}_0 H(t)$, where $\hat{\Theta}_0 = 50\ K$ is an increase of external temperature and H(t) is a Heaviside's function (Fig. 2).

Fig. 2. Fixed rigid disk loaded by external temperature

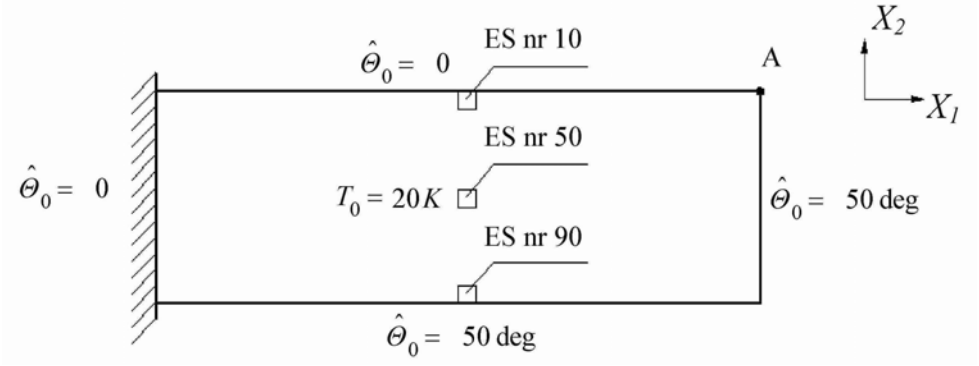

Geometrical dimensions of the rigid disk are: length l = 5.0 m, height d = 1.0 m, thickness h = 0.1 m. Rigidity of the disk is EI = 173.3(3)·10^4 kNm^2 and density of the material - ρ = 7.85 tm^{-3}. The aim of calculations is determination of the influence of non-uniform heating upon the state of displacements and stresses of the rigid disk. The rigid disk, which was divided into 100 FE, in two different periods, i.e. in time $t=1.0$ *s* by order of integration $\Delta t=0.001$ *s* and in time $t=0.1$ *s* by order of integration $\Delta t=0.0001$ *s* was observed. The deformation form of the medium surface of the rigid disk after a lapse of time $t=1.0$ *s* is presented in Fig.3. The change in time of vertical displacements of the upper right corner of the rigid disk (point A) is illustrated in Fig. 4. The distribution of normal and shearing stresses in cross sections is presented in Fig.5.

Fig. 3. Deformed shape of medium plane of the rigid disk at time *t=1.0 s*

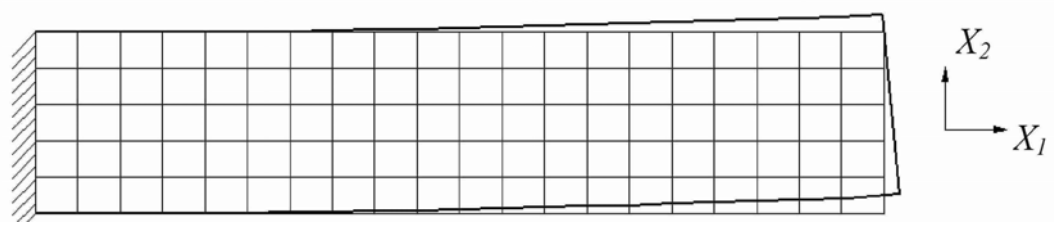

Rapid heating of the rigid disk, apart from fields of temperature, generates also fields of strains and stresses. Strains of the rigid disk are changing in an oscillatory manner. To notice this phenomenon was only possible by using a very small integration step, i.e. $\Delta t=0.0001\ s$. Stresses which dominate in the rigid disk are normal stresses along the X_1 and X_2 axes. But the shearing stresses are negligibly small. Mechanical vibrations of the rigid disk cause periodical changes of its volume. In the initial phase of the heating process, a phenomenon of simultaneous formation of tensile and compression stresses in several points of the rigid disk are observed.

Fig. 4. Time changes of vertical displacements in point A in a period *t=0÷0.1 s* with the integration step *Δt=0.0001 s*

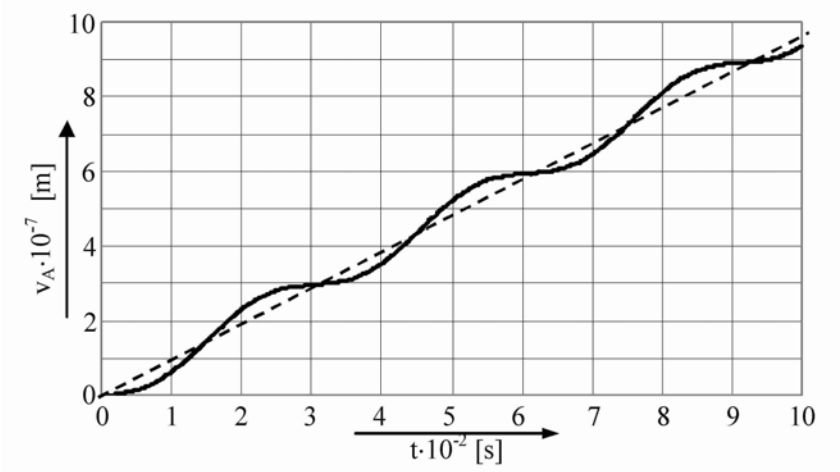

Fig. 5. Distribution of normal and shearing stresses in a section of the rigid disk at the moment *t=1.0 s*: a) near to fixed edge, b) in half of the span, c) near to free edge

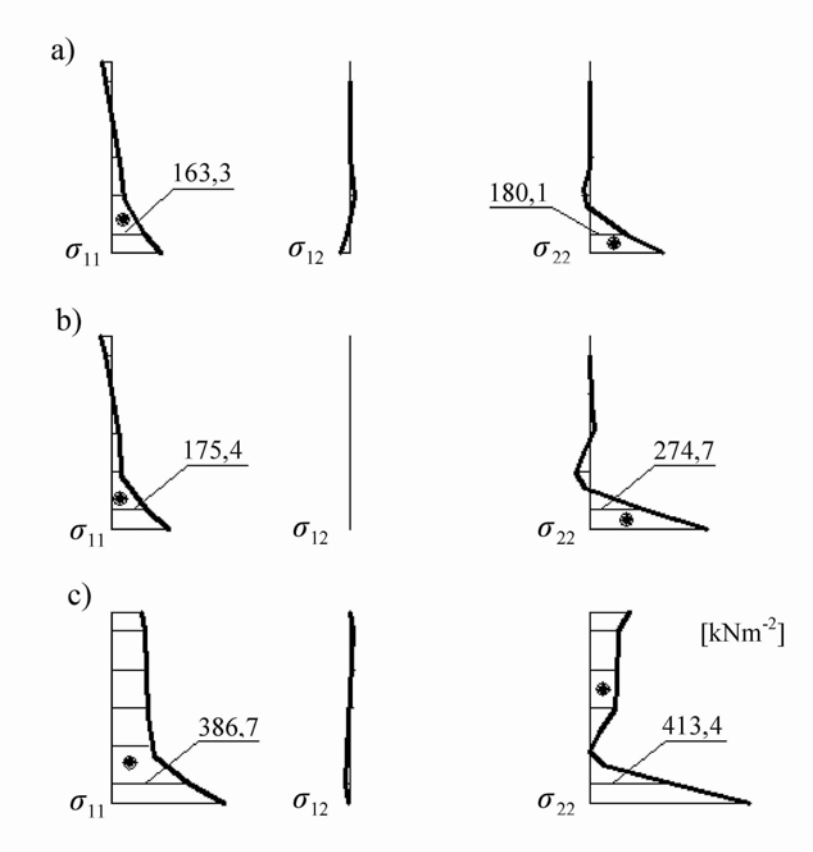

Example 2

A band of a rigid disk fixed at top, loaded rapidly with external temperature $\Theta_z(t) = \hat{\Theta}(t) = \hat{\Theta}_0 H(t)$ is considered, where $\hat{\Theta}_0 = 50\ K$ is an increase of external temperature and H(t) is Heaviside`s function (Fig. 6).

Fig. 6. Band of disk loaded by temperature

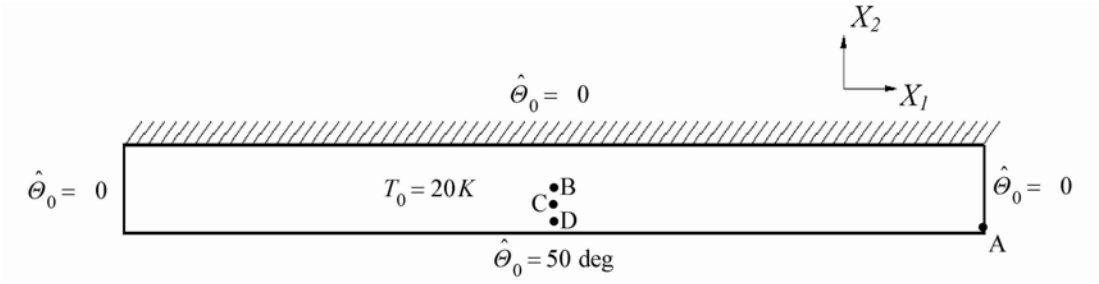

Geometrical dimensions of the rigid disk are: length l = 10.0 m, height d = 0.4 m, thickness h = 0.1 m. Rigidity of the disk is $EI = 11.093 \cdot 10^4$ kNm^2 and density of the material - $\rho = 7.85$ tm^{-3}. The rigid disk was divided into 200 FE and was observed in different periods with different integration steps successively assumed $\Delta t = 10^{-5} s$, $\Delta t = 10^{-4}\ s$, $\Delta t = 10^{-3} s$ and $\Delta t = 1.0\ s$. In Fig. 7 a change in time of the vertical displacement of the bottom right edge of the rigid disk (point A) is presented. Rapid loading with temperature at the edge of the rigid disk induces its vibration. The displacements increase in an oscillatory manner. The increase of temperature in the rigid disk is illustrated in Fig. 8. The process of heat conductivity in the rigid disk runs very slowly, nearly statically. But mechanical vibrations caused by the rapid heating of the edge of the rigid disk are quickly transmitted. These vibrations cause periodical change of the disk volume.

Fig. 7. Time changes of vertical displacements in point A

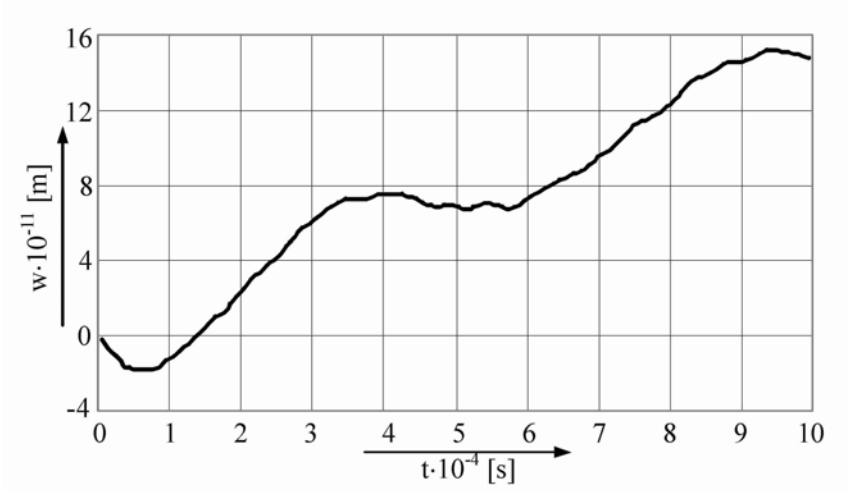

Tension of rigid disks (enlargement of volume) causes a drop in temperature, while compression (reduction of volume) – an increase in temperature. The increase of temperature in the rigid disk caused by its heating appears later and runs slowly. Figure 8 shows that in some points inside the rigid disk, a decrease of temperature in relation to initial temperature despite heating of edges appears. The reason for the temperature decrease are mechanical vibrations of the rigid disk caused by its rapid heating, which causes a temporary change of the disk volume. This phenomenon is connected with the decrease and simultaneous increase of temperature in particular points inside the disk.

Fig. 8. Increase of temperature in time

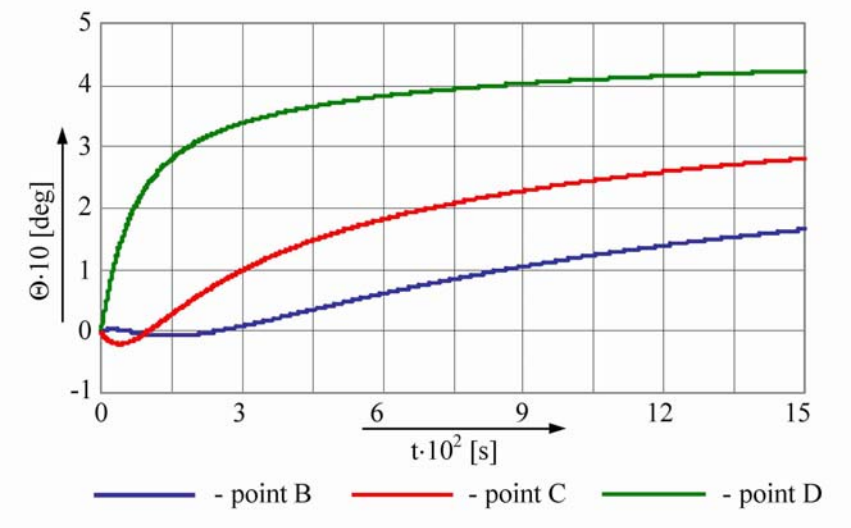

Fig. 9. Distribution of normal stresses in a cross section of the rigid disk in the half span
a) at the moment *t=1.5 s*, b) at the moment *t=600 s*

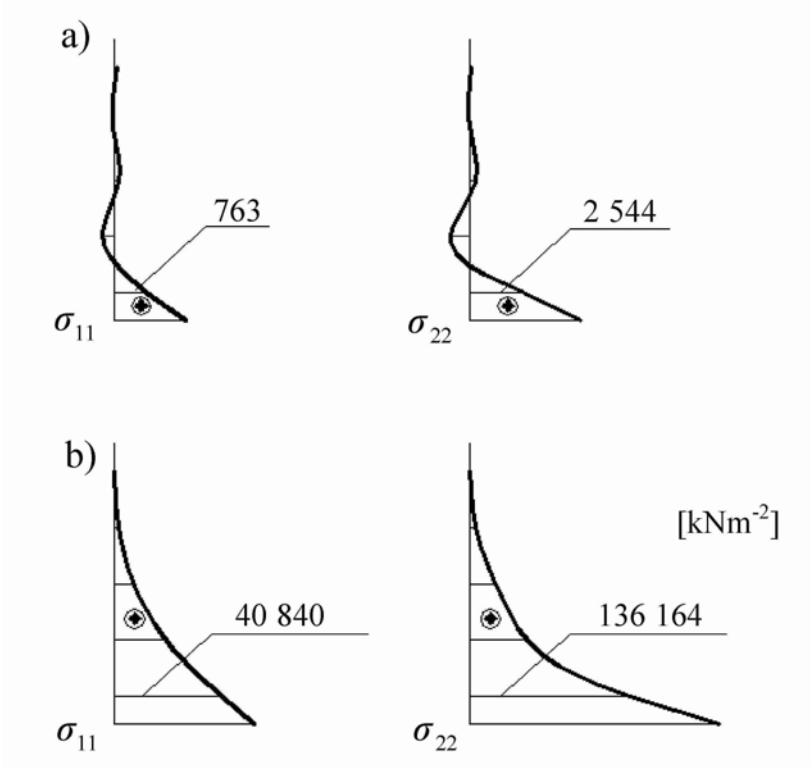

The distributions of stresses in cross- and longitudinal sections are illustrated in Fig. 9 and 10. Normal stresses in X_2 directions are dominant, but shearing stresses are negligible small. Periodical changes of the disk volume, caused by rapid heating, in some points of the disk generate tensile stresses, while in other - compression. Hence, in the diagrams illustrating distribution of normal stresses in cross sections (Fig. 9a) one can observe some disturbances. Such a phenomenon only in the initial process of rigid disk heating maybe observed, when the increase and decrease of temperature are generated by mechanical vibrations. At the moment when external thermal action causes an increase in temperature inside the rigid disk, in its all points tension appears, and in diagrams of normal stresses no local disturbances can be observed (Fig. 9b).

Fig. 10. Distribution of stresses in the longitudinal section of the disk at the moment *t= 1.5 s*

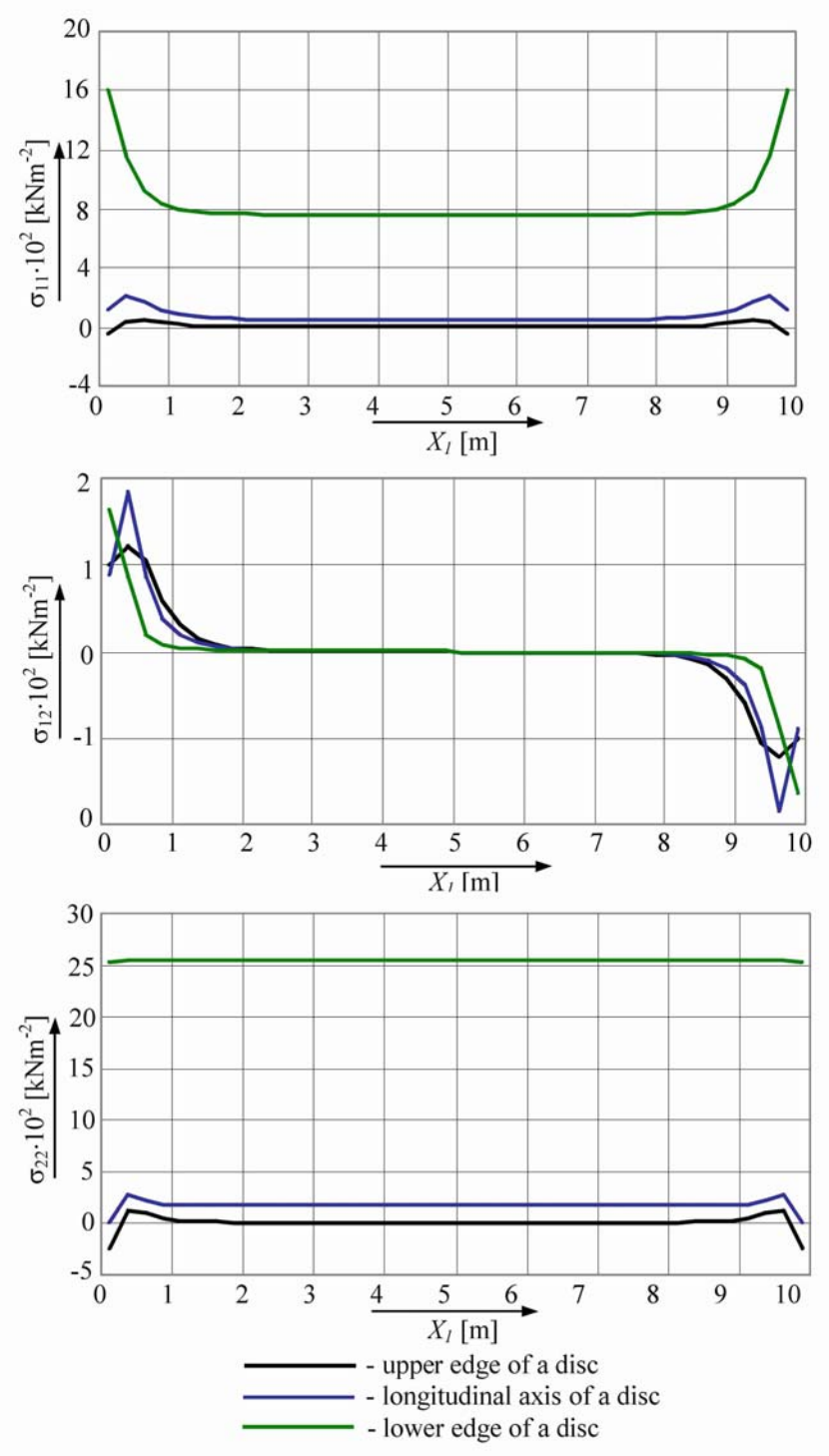

Example 3

A band of a rigid disk of the same geometry as in Example 2 is considered. The band is loaded by Heaviside`s force $p(t) = p_0 H(t)$ distributed along the bottom edge (Fig. 11), where $p_0 = 100$ kNm$^{-1}$ and $H(t)$ is Heaviside`s function.

Fig. 11. The band of rigid disk loaded by Heaviside`s force

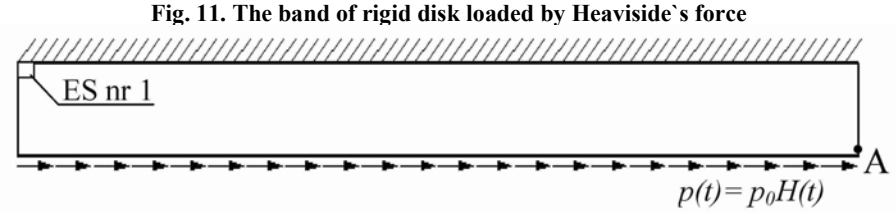

The rigid disk was observed in a period $t=1.5\ s$ with the integration steps $\Delta t=10^{-4}s$ and $\Delta t=10^{-3}s$. The external load generates in the disk, apart from fields of strains and stresses, also a field of temperature, which is changing in an oscillatory way. The change in time of horizontal displacements of the right bottom corner (point A) is presented in Fig. 12. The increase of temperature in time, near the left upper corner of the rigid disk (FE No 1) is illustrated in Fig. 13.

Fig. 12. Time changes of horizontal displacement in point A of the rigid disk

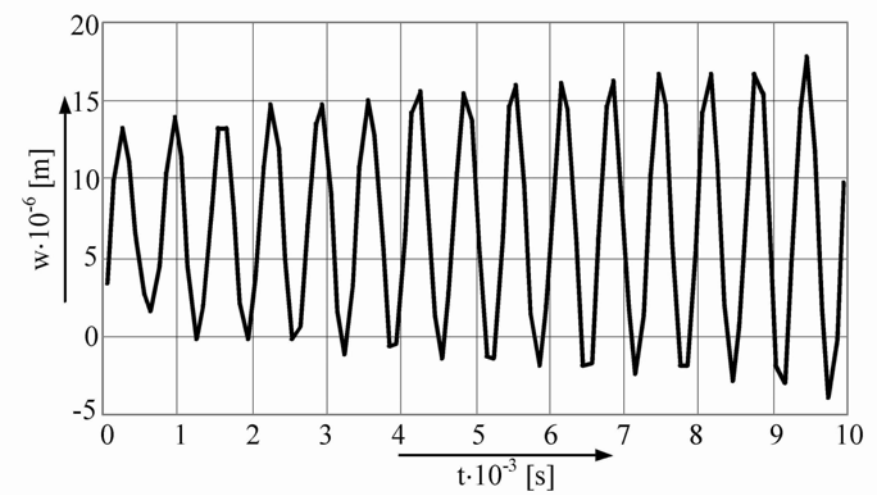

The change of temperature period is approximately equal to vibration period of the rigid disk. The analysis of distribution of normal and shearing stresses as well as temperature in longitudinal sections of the rigid disk was also considered (Fig. 14 and 15).

Fig. 13. Change of temperature of FE No 1 in time

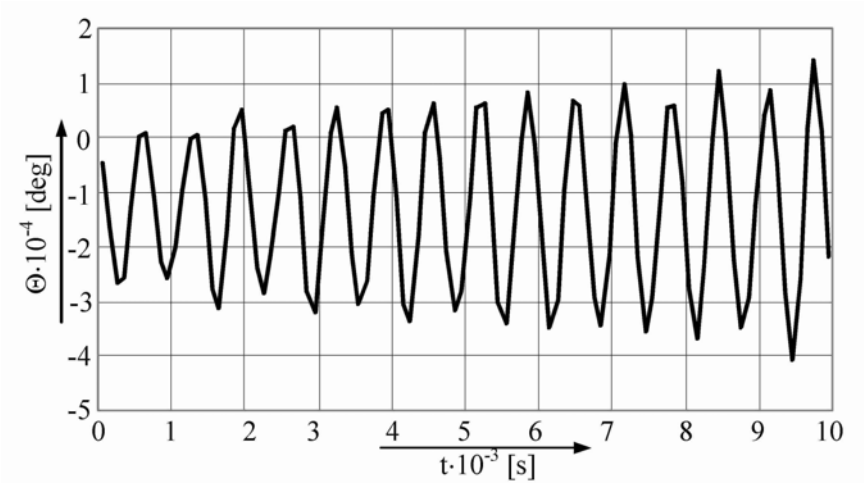

The distribution of normal stresses in longitudinal sections of the rigid disk is asymmetrical, like the distribution of temperature. When tensile stresses are generated, the temperature of the disk decreases, on the contrary - in a compressed part of the rigid disk – the temperature increases. The shearing, which distribution in longitudinal sections is symmetrical with respect to the diagonal axis of the disk is the dominant stress.

Fig. 14. Distribution of stresses in the longitudinal sections of the disk at the moment *t=1.5 s*

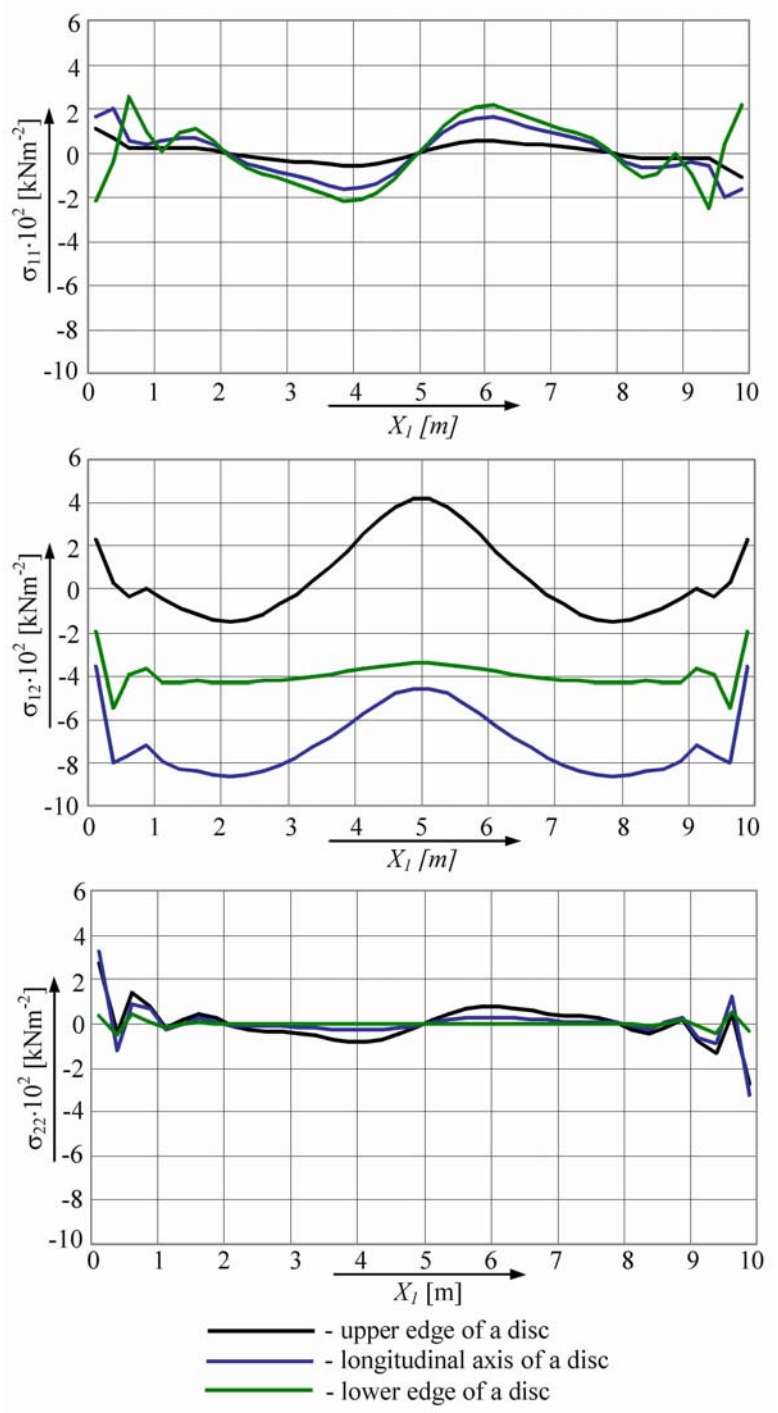

Fig. 15. Distribution of temperature in the longitudinal section of the disk at the moment *t=1.5 s*

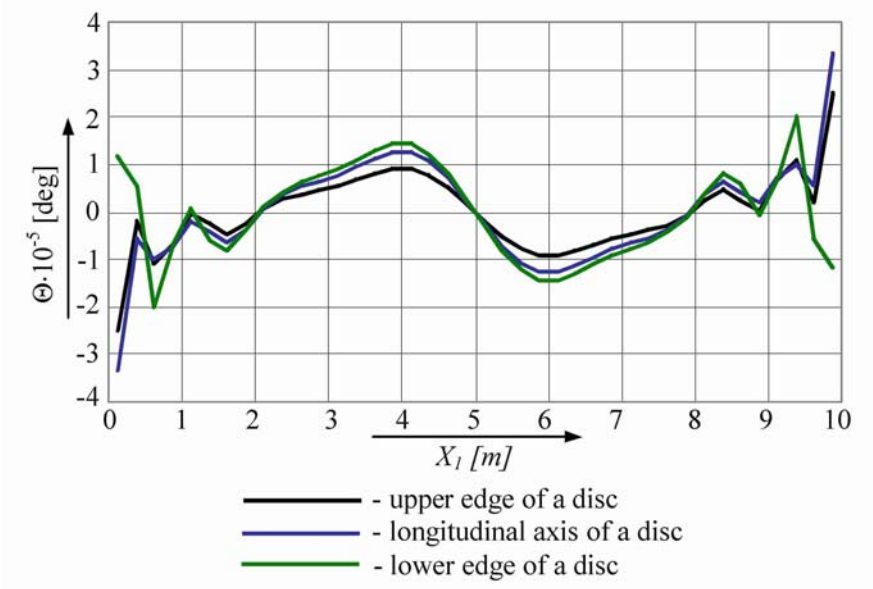

6. SUMMARY

The virtual work equations of coupled thermoelasticity were solved with two numerical methods. In the first place, a finite elements method was used, and as result of it, a set of ordinary differential equations with respect to time was obtained, which were solved with Zienkiewicz-Wooda's method (SSpj method) afterwards. After application of these methods, the initial-boundary problem was reduced to solution to two sets of algebraic equations, which with known initial conditions could be solved recurentially.

In presented examples, a rigid disk under a variable in time external load and thermal interaction was examined. An external load generates, apart from fields of strains and stresses, also a field of temperature. Under the influence of rapidly applied and released external load, these fields varied in an oscillatory manner. The thermal load also causes fields of temperature, strains and stresses. The fields of strains and stresses, under a rapid change of temperature, vary also in an oscillatory way, whereas the temperature in substance asymptotically aim at the value of external temperature acting upon the rigid disk. In such a case, a change of temperature inside the rigid disk is caused not only by external temperature but also by mechanical vibration generated by rapid heating of the disk. Mechanical vibration causes also a periodical change of the disk volume, as a result of which in some points of the rigid disk positive stresses and in another – negative stresses appear. This induces a temperature increase in some points of the rigid disk and simultaneous decrease in others parts. Observation of this phenomenon is possible only in the case, when the field of deformation and field of temperature are coupled. The used SSpj method for solving the coupled thermoelasticity appears to be very effective. A great advantage of this method is its unconditional stability with properly chosen parameters, which means that the order of integration can be, basically, selected arbitrarily. Accompanying phenomena in coupled strain-temperature fields are very subtle and possible for observations only with very small integration steps, allowed for calculations in SSpj method.

The analysed in the paper examples were calculated for a de-coupled problem as well. The influence of the field of strains with the field of temperature coupling does not exceed 1.0 % and is practically negligible. In formulation of thermoelasticity equations one assumed moderate changes of external temperature with respect to the initial temperature of the rigid disk. For considerable and rapid changes of temperature, the coupling of these fields will surely play a large role and could not be neglected. Great temperature changes may cause essential changes in parameters of materials, which would be connected with the necessity of formulation of non-linear constitutive equations and description of material parameters by functions relative to temperature.

REFERENCES

[1] Dobiszewska M., Some generalisation of the equation of virtual work in thermoelasticity. EJPAU, Electronic Journal of Polish Agricultural Universities, 1, vol. 7, 2004

[2] Zienkiewicz O. C., Wood W. L., Hine N. W., 1984. A unified set of single step algorithms, Int. I. Meth. Eng., 20, 1529÷1552.

[3] Penry S.N., Wood W.L., 1985. Comparison of some single-step methods for the numerical solution of the structural dynamics equation, Int. I. Num. Meth. Eng., 21, 1941-1955.

[4] Podhorecki A., 1997. SSpj Method of Numerical Integration Applied for Solving of Differential Equations of Viscoelastic Medium, XIII Polish Conference on Computer Methods in Mechanics, Poznań, Poland, 5-8 May 1997, 1083÷1090.

Magdalena Dobiszewska
Faculty of Building and Environmental Engineering
Technical and Agricultural Academy Bydgoszcz
ul. Prof. S. Kaliskiego 7, 85-796 Bydgoszcz
tel. 052 340-84-11
e-mail: magdalena.dobiszewska@atr.bydgoszcz.pl
